

Ab initio study of the low-temperature phases of lithium imide

Tim Mueller and Gerbrand Ceder*

Massachusetts Institute of Technology, 77 Massachusetts Avenue, Building 13-5056, Cambridge, Massachusetts 02139, USA

(Received 7 December 2007; revised manuscript received 27 October 2010; published 23 November 2010)

We present a low-temperature structural model for lithium imide (Li_2NH) that is consistent with experimental studies. Using the cluster expansion formalism and density-functional theory, we have identified a low-energy crystal structure for lithium imide with 96 atoms per unit cell. This low-energy structure is consistent with experimental diffraction patterns, and we propose that the symmetry of the structure may be increased at finite temperature due to thermal fluctuations. In addition, our results suggest that lithium motion is relatively facile between octahedral and tetrahedral sites, which may help explain how lithium diffuses through this material.

DOI: [10.1103/PhysRevB.82.174307](https://doi.org/10.1103/PhysRevB.82.174307)

PACS number(s): 61.66.Fn, 71.15.Nc, 71.20.Ps

I. INTRODUCTION

Lithium imide (Li_2NH), a potentially important material for hydrogen storage and lithium-ion conductivity,¹⁻⁵ has presented researchers with a challenging problem in structural determination. Early x-ray diffraction studies suggested that the structure of lithium imide was antifluorite, with a simple cubic sublattice of tetrahedral lithium cations and an fcc sublattice of octahedral nitrogen anions.⁶ The position of the hydrogen nuclei was not determined but several studies have presented evidence that the hydrogen is tightly bound to the nitrogen, forming imide groups.⁷⁻¹⁴ Despite extensive investigation of the structure of lithium imide, there is no consensus on the locations of the lithium nuclei or the orientations of the imide groups below approximately 360 K. Computational and experimental analyses have arrived at no fewer than eight different proposed crystal structures.⁶⁻¹⁵ In this paper, we use *ab initio* calculations along with analysis of previously reported experimental results to propose a structural model for lithium imide that is consistent with both experiments and calculated energies, and significantly more complicated than initially thought. Our result points at a unique and unexpected structural prototype for Li_2NH that may be of importance for other materials containing NH groups or other heteronuclear diatomic ions. We find that vacancies on 1/6 of the tetrahedral sites are part of the structure, which may be relevant for the kinetics of dehydrogenation and lithium-ion conductivity of this material.

In a previous paper we modeled lithium imide in an antifluorite framework,¹¹ with tetrahedral lithium cations and octahedral NH anions. Using an effective Hamiltonian for the NH group orientations, we found an antifluorite-based structure for lithium imide that has lower energy—calculated using density-functional theory (DFT) (Ref. 16)—than any proposed structure. Recent molecular-dynamics simulations indicate that lithium imide maintains a structure similar to the one we discovered at 200 K.⁴ However the simulated diffraction patterns for the proposed structure differ from those obtained experimentally (Fig. 1).^{6-8,13} In this paper we present a computational search that has obtained a structure for lithium imide that is only 17 meV/f.u. above that of the predicted antifluoritelike ground state.¹¹ The new low-energy structure is closely related to a high-symmetry structure that

is only 3 meV/f.u. higher in energy, and we propose that the experimentally observed diffraction patterns may be due to thermal fluctuations about this high-symmetry structure.

II. METHODOLOGY

Structure energies and phonon modes were calculated using the projector-augmented wave function (PAW) method¹⁷ with the Perdew-Burke-Ernzerhof¹⁸ generalized gradient approximation (GGA) to DFT as implemented in the Vienna *ab initio* simulation package (VASP).¹⁹ The standard hydrogen and nitrogen PAW potentials and *s*-valence lithium PAW potentials in VASP were used with a plane-wave cut-off energy of 500 eV. For a primitive cell calculation, total-energy convergence within 1 meV/f.u. was reached with a $7 \times 7 \times 7$ Monkhorst-Pack²⁰ *k*-point grid shifted to include the gamma point. For supercell calculations this grid was scaled down

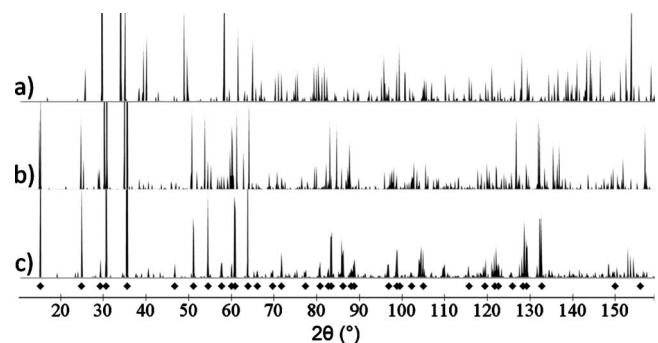


FIG. 1. The neutron powder-diffraction pattern for Li_2ND , as calculated by CRYSTALDIFFRACT, in (a) the antifluorite-based structure we previously proposed in Ref. 11, (b) the structure proposed by Herbst and Hector (Ref. 10) after removing unstable phonon modes, and (c) the structure proposed in this paper. To make comparing experimental and calculated peaks easier, we show the peaks for the structure proposed in this paper with the lattice parameter isotropically rescaled to match the resolved lattice parameter. The diamonds represent the 100 K peaks listed in Table I of Ref. 13. The wavelength is the same as that used in Ref. 13, and the tops of the highest peaks are truncated. The peak near $2\theta = 110^\circ$ is not listed in Table I of Ref. 13 but it is clearly visible in the actual diffraction plot of Fig. 2 of Ref. 13.

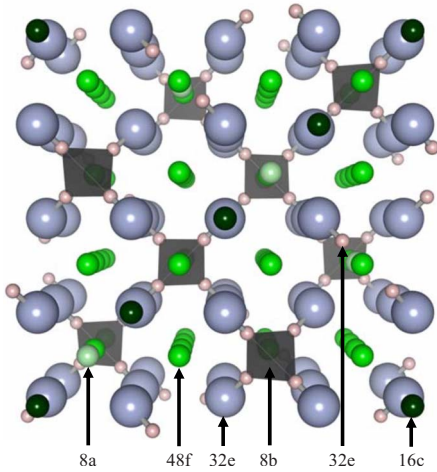


FIG. 2. (Color online) The important sites for spinel-like lithium imide structures. The large spheres represent nitrogen and the small spheres represent hydrogen. The remaining spheres represent potential lithium sites. The pale shaded (8a) are tetrahedral lithium sites that are as far as possible from the 8b vacancies. The medium shaded (48f) are tetrahedral lithium sites corresponding to the remaining tetrahedral antifluorite sites. The dark shaded (16c) are the octahedral lithium sites. In each conventional unit cell, eight of the indicated lithium sites must be vacant.

proportionately to the size of the supercell. Structures with low predicted energies were recalculated using DFT in the same manner, but with a cut-off energy of 900 eV. Vibrations were calculated within the harmonic approximation. Force constants were calculated using linear response as implemented in VASP, using supercells containing at least 128 atoms with dimensions of at least $10 \text{ \AA} \times 10 \text{ \AA} \times 10 \text{ \AA}$. Thermodynamic integration was performed using PHONOPY (Ref. 21) on an $8 \times 8 \times 8$ grid of phonon wave vectors. The identification of space groups was performed using ABINIT (Ref. 22) and the Bilbao Crystallographic Server.^{23,24}

III. APPROACH

The difficulty in finding a structure for lithium imide stems from the fact that in a close-packed lattice of nitrogen anions there are more hydrogen and lithium cations than tetrahedral sites in which to place them. Herbst and Hector have addressed this problem by proposing a structure based on a $2 \times 2 \times 2$ supercell of the conventional antifluorite unit cell.¹⁰ The structure proposed by Herbst and Hector belongs to a class of structures in which one in eight tetrahedral sites is vacant, and the N-H bonds are oriented so that four hydrogen nuclei surround each vacant tetrahedral site as shown in Fig. 2. These vacant sites are distributed the same way as the tetrahedral cations in a spinel, resulting in the same $Fd\bar{3}m$ symmetry. Because of the topological relation to spinel, structures in this class will be referred to as “spinel-like” structures. For clarity, when discussing this class of structures we will use the same origin as in Ref. 13, in which the vacant sites are the 8b sites. The remaining tetrahedral sites become the 8a and 48f sites, and the octahedral sites are labeled as 16c and 16d sites. The imide groups have a nearly

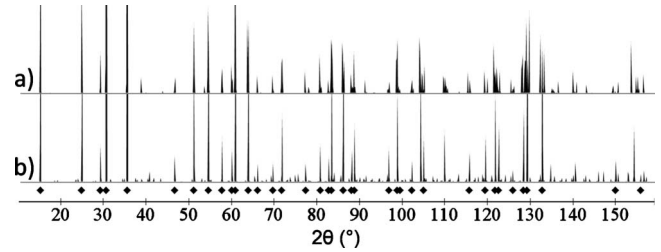


FIG. 3. The neutron powder-diffraction pattern for Li_2ND , as calculated by CRYSTALDIFFRACT, in (a) the high-symmetry structure proposed by Herbst and Hector (Ref. 10) which was determined to have unstable phonon modes and (b) the lower-energy high-symmetry structure with unstable phonon modes proposed in this paper. The experimentally observed diffraction patterns may be a result of thermal fluctuations about this high-symmetry structure. To make comparing experimental and calculated peaks easier, we show the peaks for the structure proposed in this paper with the lattice parameter isotropically rescaled to match the resolved lattice parameter. The peaks are labeled as in Fig. 1. Large green spheres represent lithium, medium blue spheres represent nitrogen, and small white spheres represent hydrogen.

face-centered-cubic arrangement, as in an antifluorite structure. In general the $Fd\bar{3}m$ symmetry is broken when the stoichiometry is restored by placing the eight displaced lithium nuclei in vacant octahedral 16c sites. In the structure proposed by Herbst and Hector, the eight displaced lithium nuclei are in alternating layers of 16c sites in the $[100]$ direction.¹⁰

While the diffraction pattern for the structure proposed by Herbst and Hector is in reasonable agreement with experiment (Fig. 3),¹³ its DFT-calculated formation energy is 50 meV/f.u. higher than the structure we proposed.¹¹ Our DFT calculations identify unstable phonon modes in this structure, and when the structure is allowed to relax along these modes (Fig. 4) the energy decreases by about 12 meV/f.u. The resulting structure has the $Pna2_1$ space group (no. 33), with lattice parameters of $a=7.23 \text{ \AA}$, $b=10.27 \text{ \AA}$, and $c=7.04 \text{ \AA}$. Site coordinates are provided in Table I. The diffraction pattern of the relaxed structure does not agree well with experiment (Fig. 1), and it is still 38 meV/f.u. higher in energy than the structure we proposed. These results make it unlikely that the structure proposed by Herbst and Hector is the correct structural model for Li_2NH unless DFT is significantly in error in this system.

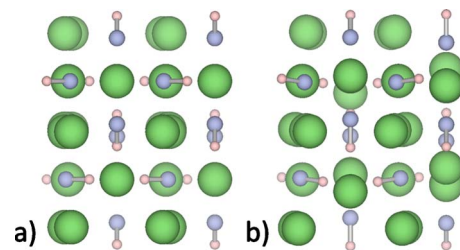


FIG. 4. (Color online) The structure proposed by Herbst and Hector (Ref. 10) (a) in the high-symmetry structure as proposed and (b) after perturbation of unstable phonon modes and relaxation. Large green spheres represent lithium, medium blue spheres represent nitrogen, and small white spheres represent hydrogen.

TABLE I. The reduced coordinates of the structure proposed in Ref. 10, after perturbing unstable modes and relaxing. The space group is $Pna2_1$ (no. 33) with lattice parameters $a=7.23$ Å, $b=10.27$ Å, and $c=7.04$ Å.

Element	Wyckoff position	X	Y	Z
Hydrogen	4a	0.2392	0.0547	0.2730
Hydrogen	4a	0.2391	0.0547	0.9865
Hydrogen	4a	0.4127	0.2356	0.1298
Hydrogen	4a	0.9162	0.6999	0.6296
Lithium	4a	0.0005	0.3874	0.6298
Lithium	4a	0.0005	0.3931	0.1297
Lithium	4a	0.0552	0.1049	0.6297
Lithium	4a	0.0552	0.2499	0.8797
Lithium	4a	0.2361	0.1187	0.8995
Lithium	4a	0.7004	0.6106	0.3414
Lithium	4a	0.3879	0.3892	0.9179
Lithium	4a	0.3936	0.8814	0.3600
Nitrogen	4a	0.1054	0.0050	0.3904
Nitrogen	4a	0.2504	0.0051	0.8691
Nitrogen	4a	0.1192	0.2381	0.6298
Nitrogen	4a	0.6111	0.7484	0.1298

Although the high-symmetry structure proposed by Herbst and Hector is unstable and relatively high in energy, it is in better agreement with experimental diffraction data than any previously proposed ordered structure. This agreement with experimental data suggests that the experimentally observed structure may belong to the same class of spinel-like structures as the Herbst and Hector structure. To find a low-energy structure for lithium imide that agrees well with experimental diffraction patterns, we search for the lowest-energy structure within this class.

To define our search space, we first develop a model for all the possible lithium and hydrogen sites in the class of spinel-like structures. The refinement of diffraction data by Balogh *et al.* suggests that the lithium ions displaced from the 8a sites are located not at the ideal 16c sites, but at nearby 32e sites between the 16c and 8a sites.¹³ The refined proximity of the two 32e sites (1.12–1.37 Å) (Ref. 13) implies they cannot be populated at the same time. For this reason, the lithium in the 32e sites can be considered to be effectively associated with a single octahedral 16c site.

The distance between the octahedral 32e site and the 8a site is between 1.50 and 1.64 Å,¹³ making it unlikely that both are simultaneously occupied. Because some octahedral site occupation by lithium is required to host lithium vacated from 8b sites, some of the 8a sites must also be vacant. Lithium occupation of octahedral 32e sites has been observed to range from 32% at 100 K to 26 % at 300 K, which was unexpectedly high and attributed to the possible existence of excess lithium in the sample.¹³ An alternative explanation may be that the excess lithium in the 32e sites comes from tetrahedral 8a lithium vacancies.

Based on the above analysis of the experimental data, a general model for the spinel-like structure of lithium imide

can be developed. The tetrahedral 8b sites are vacated by lithium and become surrounded by hydrogen, as in the structure proposed in Ref. 10. However, unlike the structure proposed in Ref. 10, the tetrahedral 8a sites may be vacant as well to accommodate the lithium displaced into the octahedral 16c sites. This leaves a large configuration space to be searched for low-energy structures which includes all possible ways in which lithium can be distributed over the 8a and 16c sites. The exploration of such a large space is infeasible with direct DFT calculations but can be accomplished by generating a cluster expansion,^{25–27} which is a lattice-model Hamiltonian that parameterizes energy as a function of the specie (or vacancy) at each site. The cluster expansion technique has been successfully used to predict different ground-state structures and phase diagrams of alloys and oxides.^{28–30} To search for the ground-state structure of lithium imide, we trained a cluster expansion on a library of 39 different decorations of 8a and 16c sites, with energies calculated using density-functional theory. This resulting cluster expansion Hamiltonian was used in a simulated annealing algorithm to identify low-energy structures.

IV. RESULTS

It was found that the system is well described by 11 clusters (Table II), with a leave-one-out cross-validation (LOOCV) score²⁶ of 4.6 meV/f.u. The most favorable interaction in the cluster expansion is a vacancy on the 8a site next to a lithium ion on the 16c site, giving further evidence of the strong lithium-lithium repulsion between these sites. The lowest-energy structures discovered using the cluster expansion were all ones in which every lithium ion on a 16c site is adjacent to a single vacant 8a site, and every vacant 8a site is surrounded by four occupied 16c sites. A second cluster expansion, with an LOOCV score of 3.5 meV, was developed to more accurately model the ordering of the vacant 8a sites under these constraints. With this cluster expansion we evaluated the predicted energies of all structures with fewer than 384 atoms per unit cell. Of these, only three structures had predicted energies within 5 meV/f.u. of the structure with lowest predicted energy. The energies for these structures were calculated using DFT, and it was found that the structure with lowest predicted energy (Fig. 5) has a DFT-calculated energy lower than that of any other known spinel-like structure.

The lowest-energy structure predicted by the cluster expansion can be created by starting with the ideal spinel-like structure shown in Fig. 2, and placing vacancies in the 8a sites of every third row of lithium ions along the [001] direction. Lithium nuclei are then placed in each of the four 16c sites around the 8a vacancies. The resulting structure relaxes to a high-symmetry structure (Table III) with the $I4_1/amd$ space group (no. 141) but to fully relax the compound and remove all imaginary phonon frequencies it is necessary to break the symmetry of this structure. The relaxed low-symmetry structure has the $Fdd2$ (no. 43) space group and is 3 meV/f.u. lower in energy than the relaxed high-symmetry structure. The lattice parameters of the conventional unit cell are $a=10.15$ Å, $b=30.54$ Å, and c

TABLE II. The clusters with nonzero ECI. The coordinates are given in terms of reduced coordinates of the conventional unit cell for the $Fd\bar{3}m$ space group with origin 2. In the cluster expansion, occupation with lithium was given a value of +1, and vacancies were given a value of -1.

Reduced coordinates of sites	Wyckoff positions	Maximum distance between sites(Å)	Multiplicity per primitive cell	ECI (meV/f.u.)
{0, 0, 0}	16c	N/A	4	9.501
{0.125, 0.125, 0.125}	8a	N/A	2	14.875
{0, 0, 0}	16c	2.201	8	5.462
{0.125, 0.125, 0.125}	8a			
{0, 0, 0}	16c	3.595	12	0.595
{0, 0.25, 0.25}	16c			
{0.125, 0.125, 0.125}	8a	4.403	4	0.228
{-0.125, -0.125, -0.125}	8a			
{0, 0, 0}	16c	6.227	24	0.872
{-0.25, -0.5, 0.25}	16c			
{0, 0, 0}	16c	7.190	12	1.053
{-0.5, -0.5, 0}	16c			
{0, 0, 0}	16c	7.190	12	0.113
{0.5, 0.5, 0}	16c			
{0, 0, 0}	16c	8.039	24	0.429
{-0.75, 0.25, 0}	16c			
{0, 0, 0}	16c	3.595	12	1.158
{0.25, 0.25, 0}	16c			
{0.125, 0.125, 0.125}	8a			
{0, 0, 0}	16c	3.595	8	0.832
{0.25, 0.25, 0}	16c			
{0, 0.25, 0.25}	16c			

=10.12 Å, and the nuclear coordinates are given in Table IV. Both the relaxed high-symmetry structure and the relaxed low-symmetry structure are shown in Fig. 5.

The simulated neutron-diffraction spectra for the different proposed structures, and experimental data from Ref. 13, are

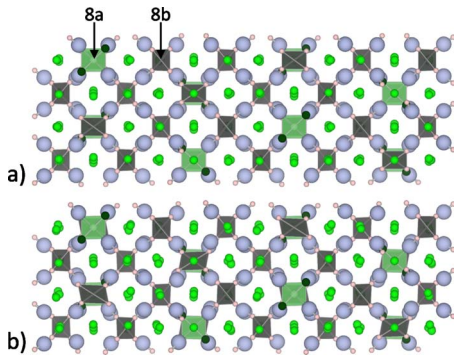


FIG. 5. (Color online) (a) The relaxed high-symmetry low-energy spinel-like structure and (b) the high-symmetry structure relaxed to remove unstable phonon modes. The spheres have the same meaning as in Fig. 2. The dark tetrahedra correspond to vacant 8b sites that are surrounded by hydrogen, and the light tetrahedra correspond to vacant 8a sites at the center of a tetrahedron of octahedral lithium (dark medium spheres). Upon relaxation the nuclei move slightly from their ideal spinel-like positions.

shown in Figs. 1 and 3. The diffraction pattern for the low-symmetry structure is similar to the experimental diffraction pattern, and the high-symmetry structure matches the experi-

TABLE III. The reduced coordinates of the unstable high-symmetry spinel-like ground state structure, in terms of space group $I 4_1/a m d$ (no. 141) with origin choice 2. $a=b=7.16$ Å, and $c=30.38$ Å.

Element	Wyckoff position	X	Y	Z
Lithium	8e	0	0.25	0.1246
Lithium	8e	0	0.75	0.0333
Lithium	8e	0.5	0.25	0.0349
Lithium	8e	0.5	0.75	0.0414
Lithium	16g	0.2715	0.0215	0.125
Lithium	16h	0.1746	0.75	0.0954
Lithium	32i	0.2685	0.5042	0.0390
Nitrogen	16h	0	0.9754	0.0882
Nitrogen	16h	0.5	0.9800	0.0817
Nitrogen	16h	0.7392	0.75	0.0022
Hydrogen	16h	0	0.0837	0.0657
Hydrogen	16h	0.5	0.3851	0.0943
Hydrogen	16h	0.8444	0.25	0.0213

TABLE IV. The reduced coordinates of the spinel-like ground state structure, in terms of space group $Fdd2$ (no. 43). $a=10.15$ Å, $b=30.54$ Å, and $c=10.12$ Å.

Element	Wyckoff position	X	Y	Z
Hydrogen	16b	0.1767	0.8967	0.2872
Hydrogen	16b	0.8346	0.8965	0.9448
Hydrogen	16b	0.1703	0.9431	0.4505
Hydrogen	16b	0.3363	0.9409	0.2913
Hydrogen	16b	0.0727	0.9615	0.0516
Hydrogen	16b	0.9347	0.9703	0.1852
Lithium	8a	0	0	0.8991
Lithium	8a	0	0	0.3496
Lithium	16b	0.4859	0.9078	0.1352
Lithium	16b	0.9756	0.9073	0.1466
Lithium	16b	0.0218	0.9119	0.8912
Lithium	16b	0.2346	0.9135	0.1036
Lithium	16b	0.7422	0.9157	0.1233
Lithium	16b	0.9983	0.9151	0.3790
Lithium	16b	0.2600	0.9164	0.8630
Lithium	16b	0.0844	0.9705	0.7121
Lithium	16b	0.4107	0.9705	0.0357
Lithium	16b	0.2497	0.0001	0.3659
Lithium	16b	0.7729	0.9996	0.1177
Nitrogen	16b	0.3670	0.8770	0.9945
Nitrogen	16b	0.1278	0.8771	0.7545
Nitrogen	16b	0.8694	0.9563	0.2521
Nitrogen	16b	0.1430	0.9579	0.9777
Nitrogen	16b	0.1109	0.9625	0.5093
Nitrogen	16b	0.3834	0.9637	0.2327

mental patterns very well. The most notable discrepancies between the experimental data and the simulated diffraction pattern for the high-symmetry structure are a slight difference in lattice parameter, and the existence of a peak near $2\theta=110^\circ$ in the simulated pattern. It is typical for GGA to produce a lattice parameter slightly larger than the experimental parameter. The peak near $2\theta=110^\circ$, while not listed in Table I of Ref. 13, is clearly visible in the actual diffraction plot of Fig. 2 of Ref. 13. The peak near $2\theta=155^\circ$ does not quite align with the experimentally observed peak, but this may be due to a continued slight overestimation of the lattice parameter. Given that the energy difference between the low-symmetry and high-symmetry structures is less than 1 meV/atom, and the atomic positions are similar in each of the structures, we propose that the experimentally observed diffraction pattern may be due to thermal fluctuations about the high-symmetry positions.

In the high-symmetry structure, the calculated distance between vacant 8a sites and the octahedral lithium is 1.54 Å, in excellent agreement with the 100 K value 1.52 Å resolved by Balogh *et al.*,¹³ considering that GGA typically underbinds. This distance is much closer to experiment than the calculated distance of 2.2–2.3 Å in the structure proposed in

TABLE V. The calculated electronic (el), zero-point (zp), and total formation energies for the structures proposed by Herbst and Hector (Ref. 10) both in the original high-symmetry form and with unstable phonon modes removed, the spinel-like structure proposed in this paper both in the high-symmetry form and with unstable phonons removed, and for the antiferroitelike structure (Ref. 11).

Structure	ΔE_{el} (kJ/mol)	ΔE_{zp} (kJ/mol)	ΔE_{total} (kJ/mol)	
			0 K	298.2 K
Reference 10, high-symmetry	-183.5	N/A	N/A	N/A
Reference 10, stable	-184.7	17.2	-167.5	-175.0
This paper high-symmetry	-186.4	N/A	N/A	N/A
This paper stable	-186.7	17.2	-169.4	-177.0
Reference 11	-188.4	17.1	-171.2	-178.7

Ref. 10. The calculated lattice parameter in the c direction for 12 layers of lithium nuclei is 30.3783 Å, or 10.1261 Å per four layers of lithium. The calculated lattice parameter per four layers of lithium nuclei orthogonal to the c direction is 10.1288 Å. These values are in good agreement with the isotropic 100 K lattice parameter of 10.0873 Å resolved by Balogh *et al.*¹³ The 32e site occupation of 33% is also in good agreement with the occupation of 32% at 100 K measured in Ref. 13.

The DFT-calculated electronic formation energy of the new spinel-like ground state, relative to Li(s), N₂(g), and H₂(g), is -1.934 eV/f.u. or -186.7 kJ/mol. This value is about 20 meV/f.u. lower than the calculated energy of the structure proposed in Ref. 10 and 17 meV/f.u. higher than the calculated energy of the antiferroitelike structure we previously proposed (Table V).¹¹ The new spinel-like ground state is the lowest-energy known structure that is consistent with experimental data. The energy difference between the spinel-like and antiferroite-like structures may be offset at positive temperatures by entropic effects, considering that the structures are quite different. To determine whether entropy may stabilize the spinel-like structure at room temperature, we have evaluated entropy due to both vibrations and lithium disorder.

The calculated difference in vibrational entropy between the two structures is slight (Fig. 6), making it unlikely that vibrational entropy stabilizes the spinel-like ground state. Configurational entropy was calculated with Monte Carlo simulations on a $6 \times 6 \times 6$ supercell of the 128-atom conventional unit cell within the cluster expansion model. The Monte Carlo simulations indicate that the structure transitions to a disordered state at about 425 K. As a consequence, the calculated configurational free energy at room temperature and below is less than 1 meV/f.u., which is not sufficient to stabilize the spinel-like ground state (Fig. 6).

In some structures used to train the cluster expansion, the lithium ions relaxed to sites other than the ones at which they started. These unstable structures do not exist in configuration space and were excluded from the Monte Carlo simula-

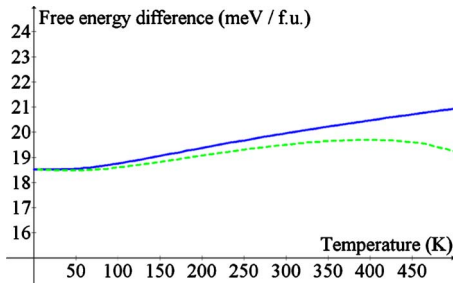


FIG. 6. (Color online) The calculated vibrational (solid blue) and combined vibrational and configurational (dashed green) free energy of the spinel-like phase relative to the vibrational free energy of the antifluoritelike structure.

tion. We found such relaxations almost always occurred whenever an 8a vacancy is adjacent to a nearest-neighbor 16c vacancy [Fig. 7(a)] or when there are nearest-neighbor 8a vacancies [Fig. 7(b)]. In both situations nearby lithium ions tend to collapse into an 8a vacancy. Because vacancies at 8a sites are unstable unless surrounded by a complete tetrahedron of occupied 16c sites, lithium nuclei to collapse from 16c sites to nearby 8a sites as the temperature is increased and these tetrahedra break up. The more tetrahedra are broken up, the more nuclei move to 8a sites, reducing the percentage of lithium on the 16c (or equivalently, 32e) sites. In the Monte Carlo simulations, the occupation of 32e sites decreases with increasing temperature to a limit of 26.1%, similar to the experimental observations in Ref. 13 (Fig. 8).

Comparison with experimental data¹³ (Fig. 8) indicates that our Monte Carlo simulations may underestimate the configurational entropy due to lithium disorder in the spinel-like structure. In addition, the low energy difference between the low-symmetry ground state and the unstable high-symmetry structure (Table V) suggests that there could be anharmonic thermal fluctuations of the atoms around their high-symmetry sites. These effects may be sufficient to stabilize the spinel-like structure near room temperature, and at lower temperatures the kinetics may be too slow for a transition to the predicted antifluoritelike ground state to be observed. The idea that lithium imide may be kinetically trapped into a particular structure at low temperatures is supported by the neutron-diffraction experiments of Yang *et al.*,

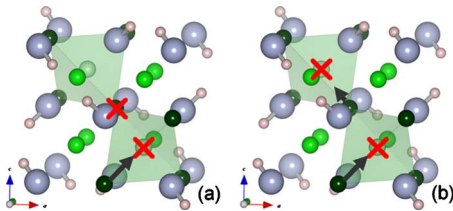


FIG. 7. (Color online) (a) The first unstable local configuration. (b) The second unstable local configuration. The large spheres represent nitrogen, the small spheres represent hydrogen, and the remaining spheres represent lithium sites. The tetrahedra have at their centers 8a sites, an on each vertex a nearest-neighbor 16c site (dark). The crosses represent vacancies, and the thick arrows show how nearby nuclei might relax.

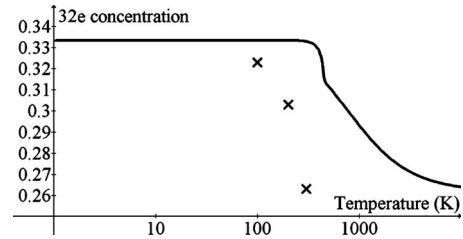


FIG. 8. A comparison of the experimental (crosses) and calculated (line) lithium occupation of the 32e sites.

who observe different diffraction patterns for lithium imide depending on the preparation temperature and method.¹⁴

V. DISCUSSION

Our new ground-state structure presents an interesting solution to the problem of where to place all the cations of lithium imide in an antifluorite structure. Conceptually, the cations remain associated with tetrahedral sites, as they would in an antifluorite structure. However, unlike antifluorite, one in six tetrahedral sites is occupied by a tetrahedral complex of four cations—four hydrogen ions in the 8b sites or four lithium ions in some 8a sites. The result is a material with a 3:1 cation to anion ratio that maintains an antifluorite-like structure. It is possible that through the mechanism of replacing a tetrahedral ion with a group of four cations lithium imide can be made off-stoichiometric. Our new structure and related disordered structures have more tetrahedral vacancies than other proposed Li_2NH structures, explaining what had been resolved to be apparently impossible proximity between lithium nuclei.¹³ To our knowledge, there is no other known structure with lower calculated energy that is consistent with experimental data. We have recently become aware that another group has arrived at a structure similar to our high-symmetry structure through *ab initio* molecular dynamics.³¹ In a separate paper, this group provides evidence of anharmonicity in the motion of the imide groups.³² These results provide further evidence that this is the experimentally observed structure.

Simulations suggest that the experimentally resolved 32e occupations are evidence of increasing configurational disorder. The 32% occupation observed at 100 K suggests there is slight disorder at this temperature (which may be kinetically frozen in). As the temperature is increased, disorder increases as well. Judging by the occupancy of the 32e site, near complete configurational disorder is reached at 300 K. Although simulations predict this should happen at a higher temperature, it is consistent with the observed spread in N-H stretching modes at room temperature³³ and the resolution of diffraction data.¹³

The experimentally observed diffraction patterns of lithium imide have been interpreted to suggest a number of different possible structures.^{6–8,13,14} We have demonstrated that to evaluate the merits of the different proposed structures and search the large multidimensional structure spaces for new structures, the use of effective Hamiltonians trained on *ab initio* calculations is an invaluable tool. By applying

this technique to the lithium imide problem we have previously predicted the existence of a distinct low-energy structure,¹¹ and in this paper we have presented a distinct structure with a 96-atom unit cell that is consistent with experimental data. We believe these results provide an interesting example of the complexity that can exist in even the most apparently simple structure determination problems.

ACKNOWLEDGMENTS

This work was funded by the Department of Energy under Grant No. DE-FG02-05ER46253. Supercomputing Resources from the San Diego Supercomputing Center are acknowledged. Crystal structures used in the figures in this text were generated using VESTA (Ref. 34).

-
- *Author to whom correspondence should be addressed. FAX: (617) 258-6534; gceder@mit.edu
- ¹P. Chen, Z. T. Xiong, J. Z. Luo, J. Y. Lin, and K. L. Tan, *Nature (London)* **420**, 302 (2002).
 - ²H. Y. Leng, T. Ichikawa, S. Hino, T. Nakagawa, and H. Fujii, *J. Phys. Chem. B* **109**, 10744 (2005).
 - ³G. P. Meisner, M. L. Scullin, M. P. Balogh, F. E. Pinkerton, and M. S. Meyer, *J. Phys. Chem. B* **110**, 4186 (2006).
 - ⁴C. M. Araujo, A. Blomqvist, R. H. Scheicher, P. Chen, and R. Ahuja, *Phys. Rev. B* **79**, 172101 (2009).
 - ⁵A. Blomqvist, C. M. Araujo, R. H. Scheicher, P. Srepusharawoot, W. Li, P. Chen, and R. Ahuja, *Phys. Rev. B* **82**, 024304 (2010).
 - ⁶R. Juza and K. Opp, *Z. Anorg. Allg. Chem.* **266**, 325 (1951).
 - ⁷K. Ohoyama, Y. Nakamori, S. Orimo, and K. Yamada, *J. Phys. Soc. Jpn.* **74**, 483 (2005).
 - ⁸T. Noritake, H. Nozaki, M. Aoki, S. Towata, G. Kitahara, Y. Nakamori, and S. Orimo, *J. Alloys Compd.* **393**, 264 (2005).
 - ⁹C. J. Zhang, M. Dyer, and A. Alavi, *J. Phys. Chem. B* **109**, 22089 (2005).
 - ¹⁰J. F. Herbst and L. G. Hector, Jr., *Phys. Rev. B* **72**, 125120 (2005).
 - ¹¹T. Mueller and G. Ceder, *Phys. Rev. B* **74**, 134104 (2006).
 - ¹²B. Magyari-Köpe, V. Ozolins, and C. Wolverton, *Phys. Rev. B* **73**, 220101 (2006).
 - ¹³M. P. Balogh, C. Y. Jones, J. F. Herbst, J. Hector, G. Louis, and M. Kundra, *J. Alloys Compd.* **420**, 326 (2006).
 - ¹⁴J. Yang, J. Lamsal, Q. Cai, W. Yelon, and W. James, *Material Research Society symposium Proceedings Vol. 1098*, MRS Symposium Proceedings (Materials Research Society, Pittsburgh, 2008), p. HH03.
 - ¹⁵G. A. Ludueña, M. Wegner, L. Bjalie, and D. Sebastiani, *ChemPhysChem* **11**, 2353 (2010).
 - ¹⁶P. Hohenberg and W. Kohn, *Phys. Rev.* **136**, B864 (1964).
 - ¹⁷P. E. Blöchl, *Phys. Rev. B* **50**, 17953 (1994).
 - ¹⁸J. P. Perdew, K. Burke, and M. Ernzerhof, *Phys. Rev. Lett.* **77**, 3865 (1996).
 - ¹⁹G. Kresse and J. Furthmüller, *Phys. Rev. B* **54**, 11169 (1996).
 - ²⁰H. J. Monkhorst and J. D. Pack, *Phys. Rev. B* **13**, 5188 (1976).
 - ²¹A. Togo, F. Oba, and I. Tanaka, *Phys. Rev. B* **78**, 134106 (2008).
 - ²²X. Gonze, J.-M. Beuken, R. Caracas, F. Detraux, M. Fuchs, G.-M. Rignanese, L. Sindic, M. Verstraete, G. Zerah, F. Jollet, M. Torrent, A. Roy, M. Mikami, P. Ghosez, J.-Y. Raty, and D. C. Allan, *Comput. Mater. Sci.* **25**, 478 (2002).
 - ²³M. I. Aroyo, A. Kirov, C. Capillas, J. M. Perez-Mato, and H. Wondratschek, *Acta Crystallogr., Sect. A: Found. Crystallogr.* **62**, 115 (2006).
 - ²⁴M. I. Aroyo, J. M. Perez-Mato, C. Capillas, E. Kroumova, S. Ivantchev, G. Madariaga, A. Kirov, and H. Wondratschek, *Z. Kristallogr.* **221**, 15 (2006).
 - ²⁵J. M. Sanchez, F. Ducastelle, and D. Gratias, *Physica A* **128**, 334 (1984).
 - ²⁶A. van de Walle and G. Ceder, *J. Phase Equilib.* **23**, 348 (2002).
 - ²⁷G. Ceder, A. F. Kohan, M. K. Aydinol, P. D. Tapesch, and A. Van der Ven, *J. Am. Ceram. Soc.* **81**, 517 (1998).
 - ²⁸A. Van der Ven, M. K. Aydinol, and G. Ceder, *J. Electrochem. Soc.* **145**, 2149 (1998).
 - ²⁹D. de Fontaine, G. Ceder, and M. Asta, *Nature (London)* **343**, 544 (1990).
 - ³⁰C. Wolverton, V. Ozolins, and A. Zunger, *Phys. Rev. B* **57**, 4332 (1998).
 - ³¹G. Miceli, M. Ceriotti, M. Bernasconi, and M. Parrinello, [arXiv:1009.1488v1](https://arxiv.org/abs/1009.1488v1) (unpublished).
 - ³²M. Ceriotti, G. Miceli, A. Pietropaolo, D. Colognesi, A. Nale, M. Catti, M. Bernasconi, and M. Parrinello, *Phys. Rev. B* **82**, 174306 (2010).
 - ³³Y. Kojima and Y. Kawai, *J. Alloys Compd.* **395**, 236 (2005).
 - ³⁴K. Momma and F. Izumi, *J. Appl. Crystallogr.* **41**, 653 (2008).